JJEES
Volume 9, (Number 2), August, 2018
ISSN 1995-6681
Pages 102 - 107
Jordan Journal of Earth and Environmental Sciences

A method for Land Degradation Monitoring in Arid and Semi-Arid Regions of Northeastern Jordan Using Landsat images

Hussam Hesham Al-Bilbisi

Geography Department, The University of Jordan, Amman 11942 Jordan

Received 27 February, 2018; Accepted 15 May, 2018

Abstract

This study evaluates land degradation in one of the most important natural grazing regions in the northeastern parts of Jordan. It describes a set of techniques that have been used to develop an operational approach that ensures high accuracy and compatibility for detecting and mapping land degradation in the study area. For this purpose, Landsat-TM and Landsat-8 images acquired in May of 2000 and May of 2014, respectively, were used. The two multi-temporal images were geometrically and radiometrically calibrated to each other, and were used for producing spatially- correct maps of environmental changes over time. Land degradation monitoring, particularly in the vegetation coverage, had been done using NDVI image differencing. The histogram of difference image shows that unchanged pixels were centered around the mean, while the changed pixels were located in the tail regions on either side. The NDVI difference image indicated that negative changes in the middle and southern parts of the study area had occurred between 2000 and 2014.

Keywords: Land degradation, arid and semi-arid, Landsat, NDVI, northeast Jordan

1. Introduction

According to the United Nation Convention to Combat Desertification (UNCCD) (UNEP, 1994), land degradation has been defined as the "Reduction or loss in arid, semi-arid and dry sub-humid areas, of the biological or economic productivity and complexity of rain-fed cropland, or range, pasture, forest and woodlands resulting from land uses or from a process or combination of processes, including processes arising from human activities and habitation patterns, such as soil erosion caused by wind and/or water, deterioration of the physical, chemical,and biological or economic properties of soil, and long-term loss of natural vegetation." It is widely accepted that the lands of arid and semi-arid regions are at the risk of degradation, most of the changes are highly dependent on the biophysical constraints of the land units (Roeder and Hill, 2009). Accordingly, the need to maintain a sustainable use of these lands entails the monitoring of the onset of land degradation so that the problem may be tackled in its early phases. Monitoring will also be required to evaluate the effectiveness of measures to control land degradation (Al-Bilbisi, 2012).

Land degradation overwhelms the whole environment; it has been a major global issue since the twentieth century and will remain high on the international agenda in the twenty-first century (Getzin, 2005; Al-Bilbisi, 2012). Land degradation is actually one of the land surface processes, which physically exhibits an increase in soil bareness and a decrease in the extent of vegetation coverage leading eventually to a reduction in land productivity. Therefore, changes of the vegetation density over time also bear important information on land degradation dynamics which are induced by natural or man-made processes. For this reason, many researchers interested in land degradation processes are concerned about the state and evolution of vegetation cover (Moody and Johnson, 2001).

Remote sensing techniques employing the output of the spectral change data provide a potential means for detecting, quantifying and monitoring changes in the vegetation cover on local, regional and global scales. Information on vegetation is generally obtained by relating vegetation indices (VIs) computed on the basis of satellite remote sensing data to pertinent variables on the terrestrial environment (Leprieur et al., 2000). There are several indices for highlighting vegetation bearing areas on a remote sensing scene; vegetation index, namely Normalized Difference Vegetation Index (NDVI) is a common and widely used index (Mbow et al., 2013; Sommer et al., 2011). It is an important vegetation index, widely-applied in research concerned with global environmental and climatic change (Mbow et al., 2013; Vogt et al., 2011).

Arid and semi-arid areas of northeastern Jordan, where livestock production is the main job for the local population, are considered among the most important natural grazing lands rich in herbaceous rain-fed and pasture plants in Jordan. These areas are increasingly coming under reduction or loss of their biological or economic productivity primarily due to human activities and/or climatic variation, which in turn lead to land degradation (Al-Bilbisi and Tateishi, 2003; Al-Bilbisi et al., 2004). The objective of this study is mapping environmental changes in the northeastern parts of Jordan based on extracted NDVI using Landsat images.

* Corresponding author. e-mail: hbilbisi@ju.edu.jo

2. Study Area

The study area is part of the northeastern desert of Jordan, known as the Northeast Jordanian Limestone Plateau (Figure 1). It is among the most important natural grazing lands in Jordan, rich in herbaceous rain-fed grazing plants, such as *Artimisia Alba* and *Rattamus*. The majority of the population in the study area are involved in livestock production. On the whole, arid to semi-arid climate conditions are dominant in the study area, with low precipitation being less than 100mm and a high potential evaporation ranging between 1500 mm/year and 2000 mm/year, which results in scarce water resources (JMD, 2013). There are noticeable seasonal temperature variations with summers tending to be hot and dry while winters are cool and wet. Mean annual maximum temperatures range between 35-41°C in July, but absolute maximum values can exceed 46°C. Temperatures might reach 0°C in winter, where the minimum annual mean temperatures decline to as low as 0-4°C in January (JMD, 2013). Occasional high intensive/low storms occur resulting in significant runoff and loss of major potential water resources due to the lack of good management and control. In summers, the wind speed ranges between four knots and six Knots, due to depressions that move along the eastern Mediterranean, while in winters, it ranges between five knots and eight knots. There are occasional gales (JMD, 2013).

The study area is a monotonous -flat plateau- and stony desert extending eastwards from the Basalt Shield beyond the eastern borders of Jordan. Small scarps formed by more resistant beds of the Tertiary sedimentary sequence occasionally interrupt it. The land rises in all directions from the eastern margin of the Basalt Shield (Figure 1). The area contains many flats, frequently more than 10 km long but rarely more than 1 km wide (Bender, 1974). Gradients are rarely steep, and there are few breaks of slope. Almost gentle concavo-convex slopes characterize the topography. The ground surface is largely covered by typical desert pavement. The soil consists mainly of limestone rocks or basalt accompanying limestone rock in some areas. According to the Soil Map of the World-Revised Legend (FAO/UNESCO, 1990), the area has mainly two dominant types, namely Gypsisols and Calcisols. Gypsisols formed in the mudflat plains (Qaa). Qaa is the local expression for the fine sediment deposits, which are formed through dissolution from calcium sulphate contained in weathering materials. Much of the drainage appears to be radial, draining to and terminating in a large Qaa. Mudflat plains (Qaa) accumulate from the ephemeral standing water through the many wadis' discharge in the mudflats plains. They comprise fine, soft, various amounts of evaporates and silty clay. The most prominent feature of Calcisols is the translocation of calcium carbonate from the surface layers to an accumulation layer at some depth in the soil. This layer may be soft and powdery, or may consist of hard concretions and can eventually become indurate and cemented. Most Calcisols have a medium to fine texture and a good water holding capacity. They are generally well- drained. These are potentially fertile soils, but their high calcium carbonate content is not favorable for many crops because it may result in iron and zinc deficiency in crops. However, these soils are used mainly for grazing (FAO, 2000).

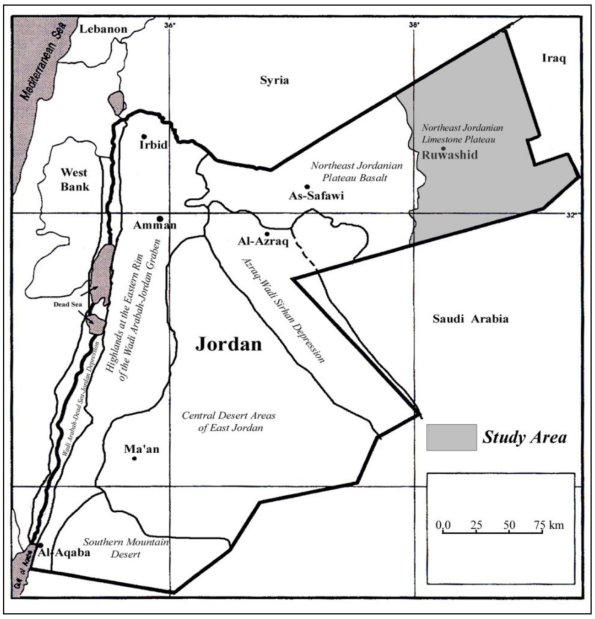

Figure 1. Jordan map showing the main geomorphological units, with the study area in gray color in the northeastern part of the country.

3. Methodology

3.1. Geometric Rectification and Radiometric Calibration

Digital images covering the study area were geometrically and radiometrically calibrated to each other to facilitate their comparison (Lillesand et al., 2014). Geometric correction is a methodology for rectifying satellite images to the same projection system. For producing a spatially-correct map of environmental changes through time, a subset of each of the Landsat TM (Figure 2) and Landsat 8 (Figure 3) digital images acquired in May of 2000, and May of 2014; respectively, were used. The 2014 Landsat 8 image, which was supplied by USGS, had already been rectified and georeferenced to UTM map projection (Zone 36N), and WGS84 datum. Then, this image was employed as the reference scene to which the second scene (TM of 2000) was registered. Using image-to-image registration, the first-degree polynomial equation was used in image transformation. The resultant root mean square error (RMSE) was less than half-pixel (15 m), indicating an excellent registration. The nearest neighbor resampling method was used to avoid altering the original pixel values of the image data.

An important component to the change detection is radiometric calibration and corrections (Chavez and Mackinnon, 1994). Radiometric calibration and corrections can eliminate or reduce the image differences introduced as a result of changing atmospheric conditions. Since both images are acquired within the same season. A histogram matching provided by PCI software was used in this study. After this correction, image statistics and histograms from the two periods were found to be similar and comparable.

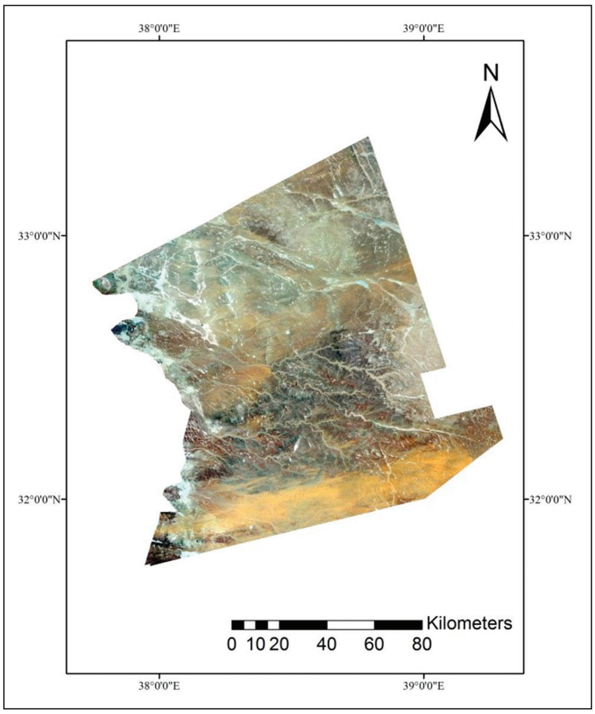

Figure 2. Color composite image of Landsat-TM (2000), bands (MIR, NIR, and Green) exposed through the red, green and blue filters, respectively.

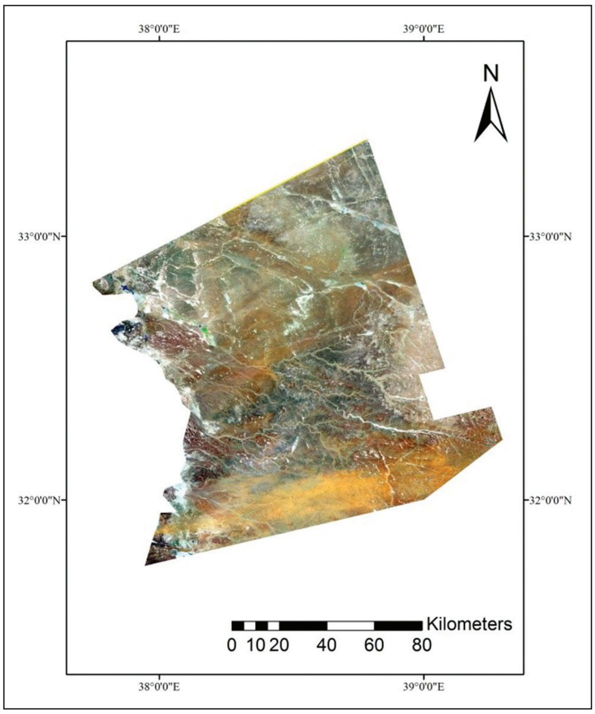

Figure 3. Color composite image of Landsat - 8 (2014), bands (MIR, NIR, and Green) exposed through the red, green and blue filters, respectively.

3.2. NDVI and Image Differencing Generated Image

To facilitate the mapping of land degradation in the arid and semi-arid regions using remote sensing technology, the physical parameters of vegetation must be accurately evaluated. For this purpose, Normalized Difference Vegetation Index (NDVI) (Rous et al., 1974) was used for monitoring land degradation in the study area. NDVI is an algorithm for monitoring vegetation using spectral information of remotely-sensed data, and it can be written as (Rouse et al., 1974):

$$NDVI = \frac{NIR - RED}{NIR + RED} \tag{1}$$

where *NIR* is the spectral response of near infra red band and *RED* is the spectral response of red band. NDVI images were generated for both dates using equation (1) for the purpose of land degradation mapping. NDVI values were expressed in digital values, and were determined as:

$$DN = (NDVI * 100) + 100 \tag{2}$$

Land degradation can be quantified in terms of: (1) soil loss (2) loss of soil quality, e.g., nutrient loss and/or soil compaction (3) a decline in vegetation (forage) production or (4) a change in vegetation species composition contrary to management goals (Pickup, 1989; Behnke and Scoones, 1994; Washington-Allen et al., 1998).

For land degradation mapping, particularly in vegetation coverage, an image differencing method was adopted for pixel-by-pixel comparison and was performed on the NDVI generated images of both dates. Image differencing was calculated as:

$$LATER\ IMAGE - FORMAR\ IMAGE + 25 \tag{3}$$

where 25 is a constant to remove negative values. Subsequently, subtracting NDVI images generated NDVI difference image.

4. Results and Discussion

4.1. Land Degradation Monitoring Using NDVI Image Differencing

This method was performed on the NDVI generated images using Formula (3) where the early image was subtracted from the later image. The resultant NDVI image does not include negative values since a constant (twenty-five) was added during the image differencing. Figure (4) shows the histogram data plot, which was extracted from the resultant image of the generated NDVI difference image.

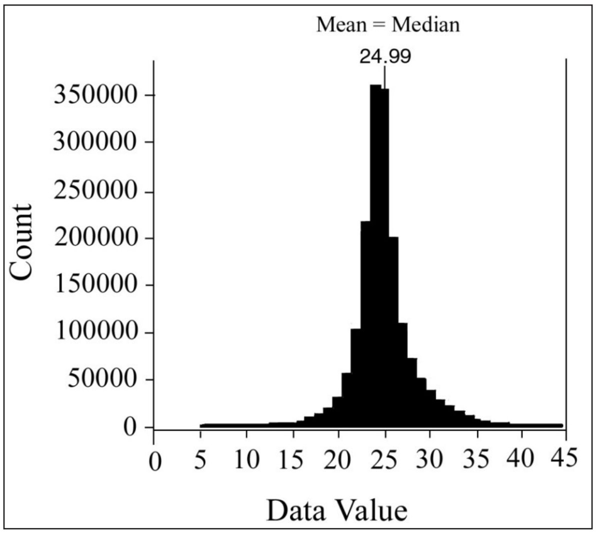

Figure 4. Histogram for the generated NDVI difference image.

When the difference image is Gaussian in nature, unchanged pixels are centered around the mean, while the tail regions on either side of the histogram contain information about the changed area (Qong and Igrashi, 1999). Misregistration is a major problem in image differencing because it may generate artifact changes during the change detection procedure. This problem can be addressed by statistical methods (Prakash and Gupta, 1998). The standard deviation of the difference image establishes a threshold level at which changes were deduced. To contain any misregistration, Singh (1989) recommended a threshold level of ± s (standard deviation) around the mean value (Singh, 1989; Washington-Allen et al., 1998, and Qong and Igrashi, 1999). For image differencing, unchanged pixel values should be equal to zero in theory (in this case it should be equal to 25). For this study, the difference image is Gaussian in nature (Figure 4), where the mean value is equal to the median value (= 24.99), and one-standard-deviation s (threshold) had been used (Washington-Allen et al., 1998, Qong & Igrashi, 1999, and Al_Bilbisi, 2012), s value is 1.15. As mentioned above, since many unchanged pixels are centered around the mean, the mean ± s (standard deviation) threshold level of the difference image was used. All pixel values within the mean ± s (near the Mean) are thus assumed to be unchanged pixels, and tail regions on both sides are assumed to contain information about the positive (gain) and negative (loss) change pixels.

The difference image was density-sliced and color-coded using the above threshold selection method to distinguish unchanged pixels from changed pixels (Figure 5). The threshold boundary between the changed pixels and unchanged pixels is determined according to the following rules, If:

- *NDVI difference image DN <= Mean + s AND >= Mean -s, then unchanged pixels.*
- *NDVI difference image DN > Mean + s, then positively changed pixels (gain).*
- *NDVI difference image DN < Mean - s, then negatively changed pixels (loss).*

The positive changes in the difference image denoted that the NDVI values of the later image were larger than the former one. Similarly, the negative values denoted that the NDVI value of the later image was smaller than the former one. Positive changes represent an increase in the vegetation cover between the two dates. Negative changes represent a decrease in the vegetation cover or a decrease in lower NDVI values. The difference image indicated that significant changes had occurred between 2000 and 2014, particularly in middle and southern parts of the study area; these areas had negative changes (Figure 5).

4.2. Main Possible Reasons of the Land Degradation in the Study Area

Based on the obtained results and the observed ground data, the main possible causes of the land degradation in the study area are:

(I) **Soil Erosion by Wind**: Soil erosion occurs when wind transports soil particles by suspension, surface creep or saltation over distances from a few centimeters to many kilometers. This depends on two factors (1) the ability of the wind to carry particles, and (2) the susceptibility of the soil surface to erosion. Wind erosion is greatest under the following conditions: scarce rainfall, high temperature, high wind velocity, and the lack of vegetation cover for significant parts of the year (CGER, 1997). Several recent studies have supported the view that wind erosion is a principal mechanism for the reduction of soil fertility in arid and semi-arid regions. Soil erosion by wind is the major reason for land degradation in the study area (Figure 6), where wind erosion caused sand drifts that covered and destructed the vegetation cover in this area.

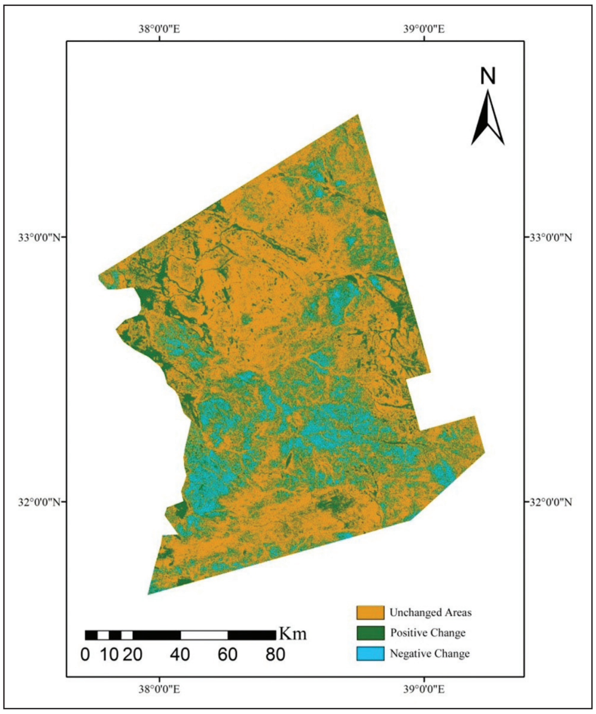

Figure 5. Density sliced NDVI difference image of the study area.

Figure 6. Sand drifts covered the vegetation in the study area.

(II) **Over-Grazing**: land degradation as a consequence of over-grazing occurred as a result of the removal of edible species which encouraged the inedible species to grow up (Figure 7). Then, if pressures continued, the modification of soil and water conditions worsen to the extent that all the vegetation gets removed and soil erosion becomes a major problem. It is clear that plant destruction is not solely achieved by eating, and the trampling of plants, the disturbance of root systems by scuffing and compaction of the surface will also reduce rainfall infiltration and all of that contributes to damage and cause the desertification.

Figure 7. Anabasis (inedible plant species) a consequence of overgrazing in the study area.

(III) **Soil Salinization**: The low rate of rainfall and the high rate of evaporation are the main causes behind soil salinization in the study area. In some areas, the surface of the soil is covered by a thin layer of calcium carbonate (Figure 8) contained in weathering materials to the extent that dry fragments do not slake in water and plant roots cannot penetrate; since salt tolerance of most plants is relatively low, therefore, the productivity rapidly declines, and as a result land degradation occurs

Figure 8. Thin layer of calcium carbonate causing soil salinization in the study area.

Conclusion

The methodology developed in this research to map land degradation using Landsat-TM and Landsat-8 images was based on an adequate understanding of the landscape features, and NDVI generating images. The NDVI image differencing method was used for land degradation monitoring, particularly in vegetation coverage. The difference image indicated that negative changes mostly in the middle and southern parts of the study area had occurred between 2000 and 2014. Based on the observed ground data, the main possible causes of the land degradation in the study area are soil erosion by wind, over-grazing and soil salinization. Therefore this area needs more attention from decision-makers to minimize the effects of land degradation in this region.

Acknowledgement

The author would like to express his great gratitude for The University of Jordan for the funding support during my sabbatical year 2014-2015 spent at Mu'tah University.

References

[1] Al-Bilbisi H. (2012). A two decades land use/cover change detection and land degradation monitoring in central Jordan using satellite images. Jordan Journal of Social Sciences, 5(1): 133-149.

[2] Al-Bilbisi, H., Tateishi R., and Tetuko, S.S.J. (2004). A technique to estimate topsoil thickness in arid and semi-arid areas of north-eastern Jordan using synthetic aperture radar data, International Journal of Remote Sensing, 25(19): 3873-3882.

[3] Al-Bilbisi, H., and Tateishi, R. (2003). Using satellite remote sensing data to detect land use/cover changes and to monitor land degradation in central Jordan. Journal of the Japan Society of Photogrammetry and Remote Sensing, 42(6): 4-18.

[4] Behnke, R.H., and Scoones, I.(1994). Rethinking range ecology: Implications for rangeland management in Africa. In Behnke R. H., Scoones, I., and Kerven, C. (eds.), Range Ecology at Disequilibrium, London: Overseas Development Institute, International Institute for Environment and Development, and Commonwealth Secretariat, London, 1-30.

[5] Bender, F. (1974). Geology of Jordan, Gebrider Borntraeger, Berlin.

[6] CGER, Center for Global Environmental Research, (1997). Databook of desertification/land degradation. National Institute forEnvironmental studies, Japan, pp 64.

[7] Chavez, P. S., JR. and MacKinnon, D. (1994). Automatic detection of vegetation changes in the southwestern United State using remotely sensed images. Photogrammetric Engineering and Remote Sensing, 60: 1025-1036.

[8] FAO (1990). Guidelines for soil description, 3rd ed., Rome, 70pp.

[9] FAO (2000). Land Cover Classification System (LCCS) - Classification concepts and user manual-. Rome, pp 179.

[10] Getzin S. (2005). The suitability of the degradation gradient method in arid Namibia. African Journal of Ecology, Volume 43 (4): 430 -351.

[11] JMD (Jordan Meteorological Department) (2013). The official web site, <http://www.jmd.gov.jo>.

[12] Lillesand, T.M., Kiefer, R.W., and Chipman, J.(2014). Remote sensing and image interpretation. 7th ed. John Wiley & Sons, Inc. New York, USA.

[13] Leprieur, C., Kerr, Y. H., Mastorchio, S., and Meunier, J. C. (2000). Monitoring vegetation cover across semi-arid regions: comparison of remote observations from various scales. International Journal of Remote Sensing, 21(2): 281-300.

Mbow, C., Fensholt, R., Rasmussen, K., and Diop, D. (2013).
[14] Canvegetation productivity be derived from greenness in a semi-arid environment? Evidence from ground-based measurements.Journal of Arid Environments, 97: 56–65.

[15] Moody, A., and Johnson, D.M. (2001). Land-surface phenologies from AVHRR using the discrete Fourier transform, RemoteSensing of Environment, 75: 305-323.

[16] Pickup, G. (1989). New land degradation survey techniques for arid Australia: Problems and prospects. Australian Rangeland Journal, 11: 74-82.

[17] Prakash, A., and Gupta, R. P. (1998). Land-use mapping and change detection in a coal mining area- Acase study in the Jharia coalfield, India. International Journal of Remote Sensing, 19: 391-410.

[18] Qong, M., and Igarashi, T. (1999). Environmental changes deduced from satellite data in arid regions- A case study in the lower reaches of the Hotan and YARKANT rivers, China, Journal of Arid Land Studies, 9: 153-167.

[19] Roeder A., and Hill J. (eds.), (2009). Advances in remote sensing and geoinformation processing for land degradation assessment. ISPRS Series. London. ISBN-10: 0415397693.

[20] Rouse, J.W., Haas, R. H., Schell, J.A., and Deering, D.W. (1974). Monitoring vegetation system in the Great Plains with ERTS. 3ed ERTS Symposium, NASA SP-351, NASA, Washington, D. C., 1: 309-317.

[21] Singh, A. (1989). Digital change detection techniques using remotely-sensed data. International Journal of Remote Sensing, 10: 989-1003.

[22] Sommer, S., Zucca, C., Grainger, A., Cherlet, M., Zougmore, R., and Sokona, Y. (2011). Application of indicator systems formonitoring and assessment of desertification from national toglobal scales. Land Degradation and Development, 22: 184–197.

[23] Tucker, C. J., Pinzon, J. E., Brown, M. E., Slayback, D. A., Pak, E.W., and Mahoney, R. (2005). An extended AVHRR 8-km NDVI data set compatible with MODIS and SPOT Vegetation NDVI data. International Journal of Remote Sensing, 26, 4485–4498.

[24] UNEP (1994). United Nations Convention to Combat Desertification, Interim Secretariat for the Convention to Combat, <http://www.unep.ch/inch.html> .

[25] Vogt, J.V., Safriel, U., Von Maltitz, G., Sokona, Y. (2011). Monitoring and assessment of land degradation and desertification: towards new conceptual and integrated approaches. Land Degradation and Development, 22: 150–165.

[26] Washington-Allen, R. A., Ramsey, R. D., Norton, B. E., and West, N.E. (1998). Change detection of the effect of severe drought on subsistence agropastoral communities on the Bolivian Altiplano. International Journal of Remote Sensing, 19: 1319-1333.